Proceedings of the ASME 2013 Summer Heat Transfer Conference
HT2013
July 14-19, 2013, Minneapolis, MN, USA

HT2013-17796

DRAFT: ANALYTIC MODELS FOR TEMPERATURE DISTRIBUTION NEAR A NANOANTENNA

Casey N. Brock
Dept. of Mechanical Engineering
Vanderbilt University
Nashville, TN 37212
Email: casey.brock@vanderbilt.edu

Greg Walker
Dept. of Mechanical Engineering
Vanderbilt University
Nashville, TN 37212
Email: greg.walker@vanderbilt.edu

Zack Coppens
Dept. of Mechanical Engineering
Vanderbilt University
Nashville, TN 37212
Email: zack.coppens@vanderbilt.edu

ABSTRACT

Thermoplasmonic structures produce highly localized temperature fields. For simplicity, researchers often use a superposition of representative spheres to model the temperature in the non-conductive region (presumably a substrate) near the metallic structures deposited on the substrate. The superposition model provides reasonable solutions, but direct comparison to experiments is difficult because local temperature variations at the nanoscale are not accessible. Moreover, the model requires several approximations. Therefore, we compare this model to other analytic models to determine the efficacy of the superposition approach in capturing temperature distributions close to the surface of the substrate and to capture realistic boundary conditions. Results indicate that a 3D analytic model can relax approximations required for the superposition model and show that the superposition model consistently over-predicts the surface temperature.

INTRODUCTION

There has been recent interest in using nanoantennas for nanoscale heat control that can be tuned remotely using light [1,2]. These localized heat sources have applications in chemical catalysis [3–5], heat-assisted magnetic recording [6,7], phononic circuitry [8], and medical therapy [9–11].

We will discuss two methods for modeling the temperature distribution in the substrate beneath a nanoantenna. The first, the Laplace matrix inversion approach [12], models the antenna as a collection of uniform metal spheres. The temperature for a single sphere is dictated by the spherical Green's function that decays as the inverse of the distance from the sphere. The temperature in the substrate is a superposition of the contribution of each sphere with a prescribed heat. The known total heat flux, Q, is distributed amongst the spheres such that each sphere has the same temperature after the superposition. The redistribution of heat generation enforces a constant temperature in the antenna that is presumed due to the high conductivity of the antenna metal.

The second method uses a 3D Green's function with a Neumann boundary condition (prescribed heat flux) at the substrate interface. The prescribed heat flux is motivated by the uniform generation within the antenna. If we think of the 3D Green's function solution as a superposition of infinitely small point sources (not spheres) continuously distributed across the antenna/substrate interfacce, then the two methods are conceptually equivalent, except the discreteness of the spherical model introduces approximations that are unnecessary in the 3D Green's function approach.

PHYSICAL SETUP

We are interested in the heat transfer into the substrate of the nanoantenna. The substrate (thermal conductivity k_2) is immersed in a fluid (thermal conductivity k_1) and the antenna is attached to the substrate (see Fig. 1). For the foregoing analysis, we assume that the thermal conductivity of the fluid is much smaller than the thermal conductivity of the antenna of the substrate. Therefore, all the energy generated is dissipated into the substrate.

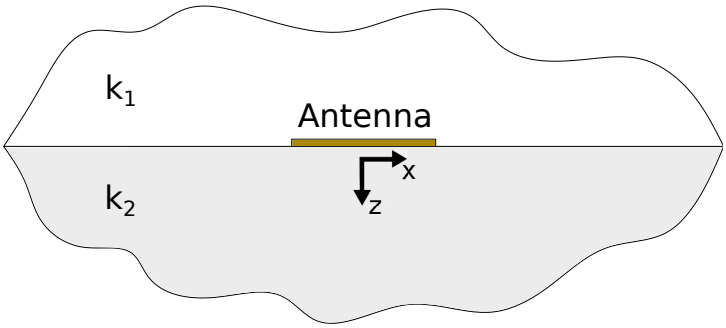

FIGURE 1. THE ANTENNA IS ATTACHED TO A SUBSTRATE (THERMAL CONDUCTIVITY k_2) WHICH IS IMMERSED IN A FLUID (THERMAL CONDUCTIVITY k_1).

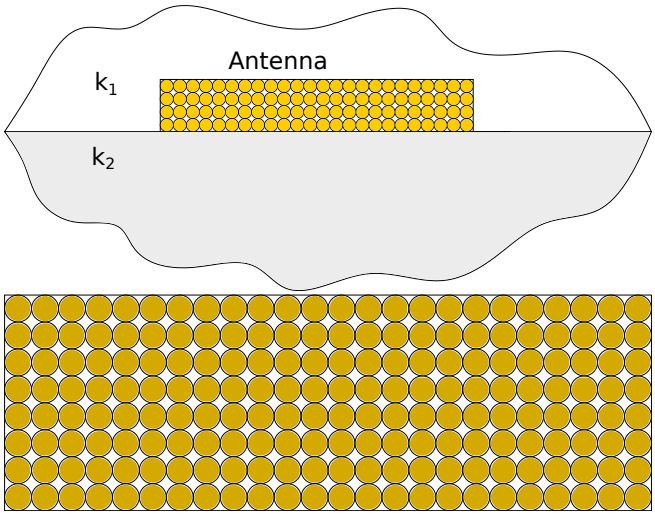

FIGURE 2. **TOP:** THE PHYSICAL SETUP FOR THE LAPLACE MATRIX INVERSION METHOD. THE SPHERES ARE ALL THE SAME TEMPERATURE. **BOTTOM:** TOP VIEW OF A DIPOLE NANOANTENNA REPRESENTED AS A COLLECTION OF SPHERES. IN THE BAFFOU PAPER [12] THE SPHERES ARE ARRANGED IN A HEXAGONAL PATTERN, BUT WE USED A RECTANGULAR PATTERN THAT WAS MORE SUITABLE FOR THIS GEOMETRY.

LAPLACE MATRIX INVERSION

The Laplace Matrix Inversion (LMI) method [12] models the antenna as a collection of metal spheres (see Fig. 2). *A fundamental assumption of this method is that the spheres are all uniform temperature.* This is justified by the high thermal conductivity of a metal antenna. If the total heat flux, Q, from the antenna is known, it can be distributed amongst the spheres so the the resultant temperature of each sphere is the same. The creation of this "fictive" heat flux is outlined in more detail by Baffou et al. [12]. If the heat flux is distributed uniformly or even according to realistic data, superposition will almost always result in a non-uniform temperature distribution in the antenna. As found by solving Laplace's equation, the temperature distribution for a solid conducting sphere is given by

$$T(\boldsymbol{r},\boldsymbol{r}_i) = \begin{cases} \dfrac{Q}{4\pi k\,|\boldsymbol{r}-\boldsymbol{r}_i|} & \text{for } |\boldsymbol{r}-\boldsymbol{r}_i| \geq a \\ \dfrac{Q}{4\pi k a} & \text{for } |\boldsymbol{r}-\boldsymbol{r}_i| \leq a \end{cases} \tag{1}$$

where a is the radius of the sphere. This solution is actually the spherical Green's function (point source) that has been truncated at the sphere surface. This solution methodology begs the question of whether the overall temperature distribution is dependent on the sphere size. The heat generation Q will increase with the cube of the sphere radius. But the inverse relationship with the sphere radius results in a net increase in temperature with the square of sphere radius. It is not clear that after superposition, the temperature away from the sphere is independent of the size of the sphere chosen. This involves the Green's function for the Laplace equation in spherical coordinates [],

$$G(r,a) = \begin{cases} \dfrac{-1}{4\pi r} & \text{for } r \geq a \\ \dfrac{-1}{4\pi a} & \text{for } r \leq a \end{cases} \tag{2}$$

Using the method of images, the Green's function for a sphere in the presence of a substrate is

$$G(\boldsymbol{r},\boldsymbol{r}_i) = \frac{1}{4\pi k_1}\frac{1}{R}\left(\frac{2k_2}{k_2+k_1}\right) \quad \text{for} \quad z \geq 0 \tag{3}$$

where

$$R = \sqrt{(x-x_i)^2+(y-y_i)^2+(z-d)^2} \tag{4}$$

and d is the distance of the sphere from the substrate. The internal temperature at the center of a single sphere is then

$$T_i = \frac{1}{4\pi k}\sum_{j=1}^{N}\left[\frac{1}{|\boldsymbol{r}_i-\boldsymbol{r}_j|} - \frac{k_2-k_1}{k_2+k_1}\frac{1}{|\boldsymbol{r}_i-\boldsymbol{r}_j^*|}\right] q_j \tag{5}$$

where $\boldsymbol{r}_j^* = \sqrt{x_j, y_j, -z_j}$ and q_j is the heat flux from sphere j. If we let all T_i be equal, we have a linear system of equations for the heat flux of each sphere. With the heat flux of each sphere,

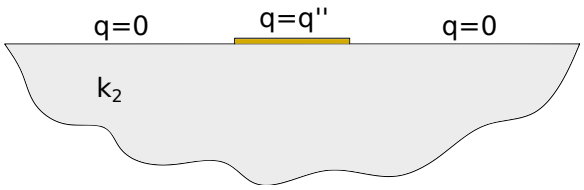

FIGURE 3. THE PHYSICAL SETUP FOR THE 3D GREEN'S FUNCTION APPROACH. THE HEAT FLUX IS CONSTANT AT THE ANTENNA/SUBSTRATE INTERFACE.

we can then use superposition to find the temperature at a given point. For a better comparison with the 3D Green's function method, we let $k_1 = 0$. An isolated sphere can have a uniform temperature, but multiple spheres in the same region can not. For example, a single sphere has a uniform interior temperature, but a second sphere in the vicinity will increase the temperature of the first sphere non-uniformly. With this in mind, the goal of LMI is to create a fictive heat source distribution such that the *centers* of each sphere are the same temperature.

3D GREEN'S FUNCTION APPROACH

In the second method, we are assuming a known heat flux, $q''(x,y)$, at the antenna/substrate interface and no heat transfer between the substrate and the fluid. These assumptions are valid as long as the thermal conductivity of the antenna is much greater than that of the substrate and the thermal conductivity of the substrate is much greater than that of the fluid. With these assumptions, we can model this as a half-space with a Neumann boundary condition at the dividing plane (see Fig. 3). The Green's function for the heat equation in this geometry is

$$G(x,y,z,t|x_0,y_0,z_0,\tau) = \frac{(e^{-\sigma_1}+e^{-\sigma_2})}{[4\pi\alpha(t-\tau)]^{3/2}} \tag{6}$$

where

$$\sigma_1 = \frac{(x-x_0)^2+(y-y_0)^2+(z-z_0)^2}{4\alpha(t-\tau)},$$
$$\sigma_2 = \frac{(x-x_0)^2+(y-y_0)^2+(z+z_0)^2}{4\alpha(t-\tau)},$$

and α is the thermal diffusivity of the substrate. The temperature at a given point is is then

$$\theta(x,y,z,t) = \frac{\alpha}{k_2}\int_{-\infty}^{\infty}\int_{-\infty}^{\infty}\int_0^t q''(x_0,y_0)\,G|_{z_0=0}\;\,d\tau\,dx_0\,dy_0\,. \tag{7}$$

In our case, q'' is the total heat flux, Q, divided by the area of the antenna if x_0 and y_0 are in the antenna region.

To develop a solution we first integrate over τ. Letting $\xi(x_0,y_0) = (x-x_0)^2+(y-y_0)^2+z^2$ to consolidate the spatial information,

$$G|_{z_0=0} = 2[4\pi\alpha(t-\tau)]^{-3/2}\exp\left(-\frac{\xi}{4\alpha(t-\tau)}\right). \tag{8}$$

The time integral in equation 7 can be performed with a change of variable, $\eta = \sqrt{\xi/4\alpha(t-\tau)}$:

$$\int_0^t G|_{z_0=0}\,d\tau = \frac{1}{\pi^{3/2}\alpha\sqrt{\xi}}\int_{\eta(\tau=0)}^{\infty}\exp(-\eta^2)d\eta \tag{9}$$
$$= \frac{1}{2\pi\alpha\sqrt{\xi}}\,\mathrm{erfc}\left(\sqrt{\tfrac{\xi}{4\alpha t}}\right). \tag{10}$$

The temperature distribution then becomes

$$\theta(x,y,z,t) = \tfrac{1}{2\pi k}\int_{-\infty}^{\infty}\int_{-\infty}^{\infty} q''(x_0,y_0)\,\tfrac{1}{\sqrt{\xi}}\,\mathrm{erfc}\left(\sqrt{\tfrac{\xi}{4\alpha t}}\right)\,dx_0\,dy_0\,. \tag{11}$$

These spatial integrals can be evaluated numerically using standard quadrature. Care must be taken at $\xi = 0$, where the integrand is infinite. This routine is set up to ignore the singularity, so $G|_{\xi=0} = 0$. This is only an issue at the antenna/substrate interface.

RESULTS

For this project, we modeled a dipole nanoantenna with a silicon-dioxide substrate ($k_2 = 1.38\,\mathrm{W/mK}$) in vacuum. The antenna is rectangular ($300\,\mathrm{nm}\times 100\,\mathrm{nm}\times 50\,\mathrm{nm}$). The total heat transfer, Q, from the antenna is $0.1\,\mu\mathrm{W}$.

For the LMI method, the fictive heat flux distribution was calculated so that the spheres were each at the same temperature and the total heat transfer, Q, from the antenna was $0.1\,\mu\mathrm{W}$. The resultant temperature distributions under the antenna in the substrate are shown in Figs. 4 and 5.

For the 3D Green's Function method, the total heat transfer, Q, is distributed evenly throughout the antenna. The resultant temperature distributions in the substrate are shown in Figs. 6 and 7. The results from each method are almost indistinguishable far away from the antenna, but the 3D Green's function approach seems to give a steeper gradient near the antenna. Moreover, the maximum temperature calculated using the 3D Green's function is significantly higher than the that of the LMI method.

A simplified analysis

Both methods gave a temperature increase of about $0.2\,\mathrm{K}$ near the antenna/substrate interface. We can also estimate ΔT

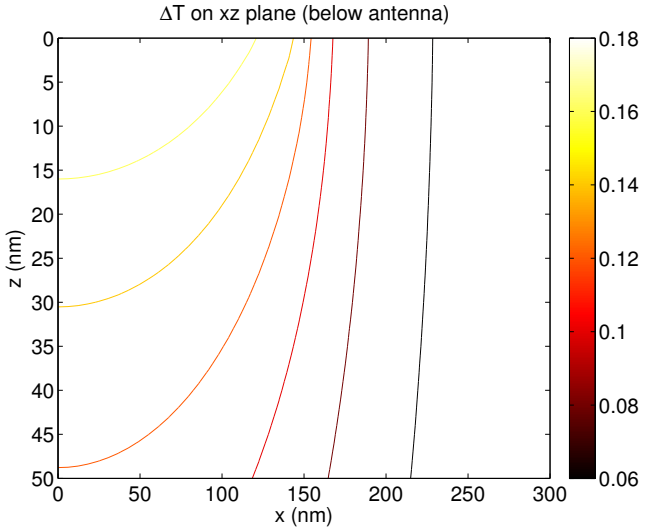

FIGURE 4. ΔT(K) BELOW THE DIPOLE ANTENNA AS CALCULATED BY THE LMI METHOD WITH $n = 4$

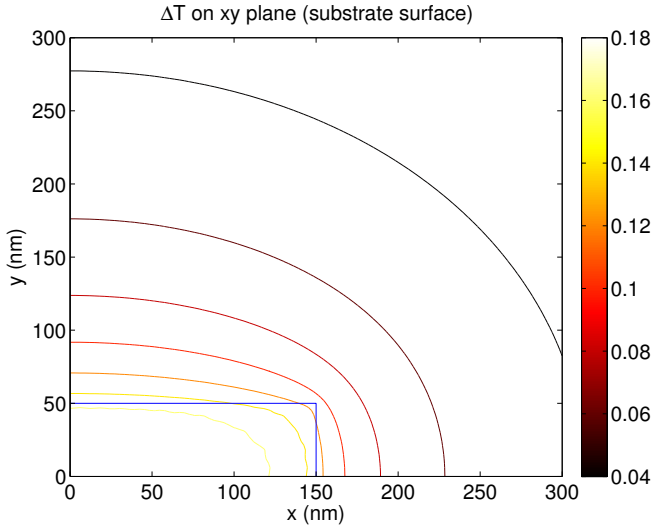

FIGURE 5. ΔT(K) AT THE SUBSTRATE SURFACE AS CALCULATED BY THE LMI METHOD WITH $n = 4$. THE RECTANGLE REPRESENTS THE POSITION OF THE ANTENNA.

using shape factors.

$$\Delta T = \frac{QL_c}{kA_s q_s} \tag{12}$$

where $A_s = 2L_xL_y$, $L_c = A_s/4\pi$, and $q_s = 0.932$ [13]. For our setup, $\Delta T = 0.1791\,\mathrm{K}$. This is reasonably close to the both the 3D Green's function result ($\Delta T = 0.2153$) and the LMI result

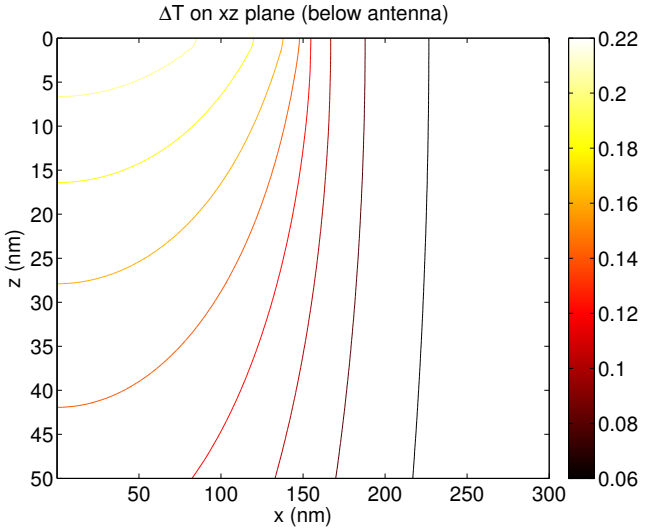

FIGURE 6. STEADY STATE ΔT(K) BELOW THE DIPOLE ANTENNA AS CALCULATED BY THE 3D GREEN'S FUNCTION METHOD

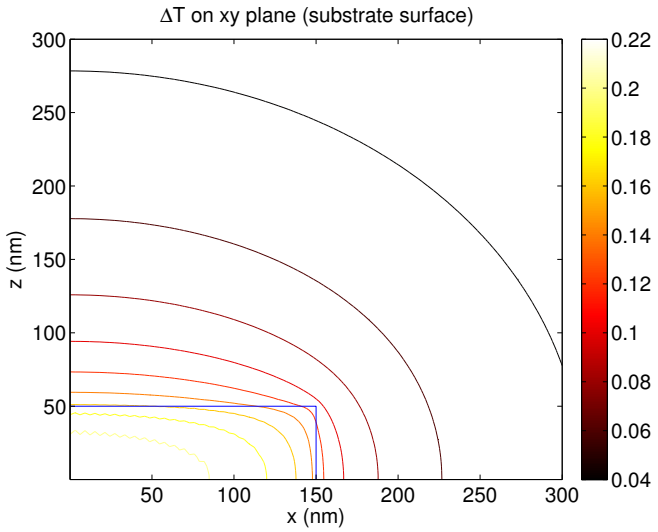

FIGURE 7. ΔT(K) AT THE SUBSTRATE SURFACE AS CALCULATED BY THE 3D GREEN'S FUNCTION METHOD. THE RECTANGLE REPRESENTS THE POSITION OF THE ANTENNA.

($\Delta T = 0.2033$).

The effect of sphere size on the LMI solution is not yet clear. The rectangular antenna has a ratio of 1:2:6 so the sphere size can be adjusted to fit more small spheres, or less large spheres in the z-direction. For example, if the number of spheres $n = 1$, there are $1 \times 2 \times 6 = 12$ spheres total, and the sphere radius a is 1/2 height of the box. If $n = 4$, there are $4 \times 8 \times 24 = 768$

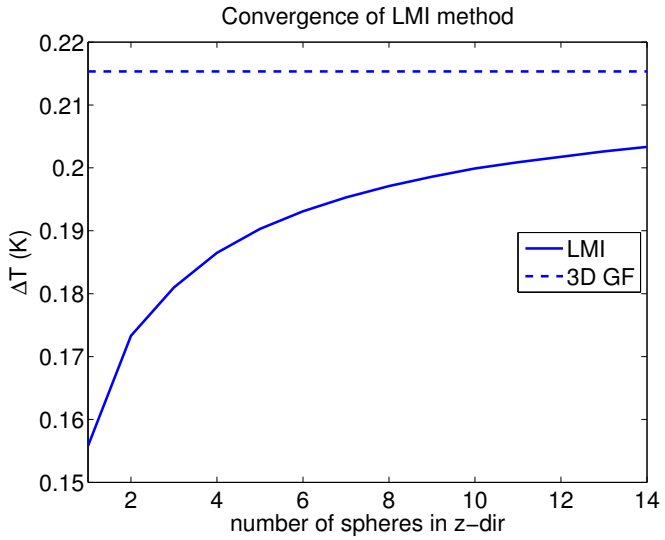

FIGURE 8. TEMPERATURE RISE AT (0,0,0) AS CALCULATED BY THE LMI METHOD FOR VARIOUS SPHERE SIZES. THE FINAL SOLUTION GIVEN BY THE 3D GREEN'S FUNCTION METHOD ($\Delta T = 0.2153$) IS SHOWN FOR COMPARISON.

spheres as shown in Fig. 2. We calculated the temperature at the point (0,0,0) as sphere size decreased (see Fig. 8). It appears that the solution is not converged even at $n = 14$ (32,928 spheres). Keep in mind that this method requires solving a system of $12n^3$ equations, which can become very computationally expensive.

CONCLUSION

The LMI method, which is an approximate solution for a constant-temperature boundary condition, is easy to implement and provides decent estimates for the steady-state temperature response in a substrate and fluid surrounding an antenna. However, arbitrary antenna designs could be difficult to discretize and the convergence of any discretized solution is dubious. The 3D Green's function approach, which is an exact solution for a constant-flux boundary condition, is easily extended to arbitrary 2D antenna designs and can naturally provide transient response as well as steady-state solutions. Moreover, the 3D Green's function approach does not have the convergence issues associated with a discretized solution.

REFERENCES

[1] Baffou, G., Quidant, R., and De Abajo, F. J. G., 2009. "Nanoscale control of optical heating in complex plasmonic systems". *ACS Nano,* ***9***, pp. 4417–4423.

[2] Govorov, A. O., and Richardson, H. H., 2007. "Generating heat with metal nanoparticles". *Nano Today,* ***2***, pp. 30–38.

[3] Aldeman, J. R., Boyd, D. A., Goodwin, D. G., and Psaltis, D., 2009. "Heterogeneous catalysis mediated by plasmon heating". *Nano Letters,* ***9***, pp. 4417–4423.

[4] Cao, L., Barsic, D. N., Guichard, A. R., and Brongersma, M. L., 2007. "Plasmon-assisted local temperature control to pattern individual semiconductor nanowires and carbon nanotubes". *Nano Letters,* ***7***, pp. 3523–3527.

[5] Christopher, P., Xin, H., and Linic, S., 2011. "Visible-light-enhanced catalytic oxidation reactions on plasmonic silver nanostructures". *Nature Chemistry,* ***3***, pp. 467–472.

[6] Challener, W. A., Peng, C., Itagi, A. V., Karns, D., Peng, W., Peng, Y., Yang, X., Zhu, X., Gokemeijer, N. J., and Hsia, Y.-T., 2009. "Heat-assisted magnetic recording by a near-field transducer with efficient optical energy transfer". *Nature Photonics,* ***3***, pp. 220–224.

[7] Stipe, B. C., Strand, T. C., Poon, C. C., Balamane, H., Boone, T. D., Katine, J. A., Li, J.-L., Rawat, V., Nemoto, H., and Hirotsune, A., 2010. "Magnetic recording at 1.5 Pb m^{-2} using an integrated plasmonic antenna". *Nature Photonics,* ***4***, pp. 484–488.

[8] Wang, L., and Li, B., 2008. "Thermal memory: A storage of phononic information". *Physical Review Letters,* ***101***, p. 267203.

[9] Jain, P. K., El-Sayed, I. H., and El-Sayed, M. A., 2007. "Au nanoparticles target cancer". *Nano Today,* ***2***, pp. 18–29.

[10] Loo, C., Lowery, A., Halas, N., West, J., and Drezek, R., 2005. "Immunotargeted nanoshells for integrated cancer imaging and therapy". *Nano Letters,* ***5***, pp. 709–711.

[11] Huschka, R., Zuloaga, J., Knight, M. W., Brown, L. V., Nordlander, P., and Halas, N. J., 2011. "Light-induced release of dna from gold nanoparticles: nanoshells and nanorods". *Journal of American Chemical Society,* ***133***, pp. 12247–12255.

[12] Baffou, G., Quidant, R., and Girard, C., 2010. "Thermoplasmonics modeling: A Green's function approach". *Physical Review B,* ***82***, p. 165424.

[13] Incropera, F. P., and DeWitt, D. P., 2002. *Introduction to Heat Transfer*, 4 ed. John Wiley and Sons.